

“Green” composites and nanocomposites from soybean oil[☆]

Zengshe Liu^{*}, Sevim Z. Erhan

Food and Industrial Oil Research Unit, NCAUR, ARS, USDA, 1815 N. University Street, Peoria, IL 61604, USA

Received 6 June 2006; received in revised form 7 December 2006; accepted 10 December 2006

Abstract

In this study, we report preparation of epoxidized soybean oil (ESO)-based “green” composites and nanocomposites. The high strength and stiffness composites and nanocomposites are formed through flax fiber and organoclay reinforcement. The epoxy resin, 1,1,1-tris(*p*-hydroxyphenyl)ethane triglycidyl ether (THPE-GE) is used as a co-matrix for flax fiber-reinforced composites. For the clay-reinforced nanocomposites, the dispersion of the clay layers is investigated by X-ray diffraction (XRD) and by transmission electron microscopy (TEM). XRD and TEM data reveal that the intercalated structure of ESO/clay nanocomposites has been developed. Mechanical properties of both materials are investigated. As curing agent, triethylenetetramine (TETA) is used for both systems.

Published by Elsevier B.V.

Keywords: Green composites; THPE-GE; Triethylenetetramine

1. Introduction

During the last few years, there has been a growing interest in the use of polymers obtained from renewable resources because advantages of these polymers include their low production cost, in some cases, and their possible biodegradability [1]. Among products from agricultural resources, natural oils may constitute raw materials useful in polymer synthesis. In order to improve the stiffness and mechanical properties of bio-based polymers for engineering applications, composite materials are prepared by the addition of reinforced particles or fibers to the polymeric matrices. Glass fiber, carbon fiber and natural fiber such as flax, pulp and hemp are used as the reinforcement of polymeric matrices. Flax has been considered as cost-effective alternative to glass in composites, since new technology and separation techniques have lowered the costs to produce fibers that are more uniform in color, strength, length and fineness and thus better suited to composites [2]. Also clay is an inexpensive natural mineral so it has been used as filler for rubber and plastic for many years, but its reinforcing ability is poor so it can only be used for conventional microcomposites. A new way to improve

the reinforcing ability of clay has been found [3,4]. Clay can be chemically modified to make the clay complexes compatible with organic monomers and polymers.

The purpose of this work is to prepare the epoxidized soybean oil (ESO)-based composites reinforced with flax fibers and nanocomposites reinforced with organoclay. Nanoreinforcement of bio-based polymers with organoclay can create new value-added applications of “green” polymers in the materials world.

2. Experimental

2.1. Forming of composites and nanocomposites

ESO and 1,1,1-tris(*p*-hydroxyphenyl)ethane triglycidyl ether (THPE-GE) (chemical structure as shown in Fig. 1) were mixed in the ratio of 1:0.33 (by weight) at 55 °C for 30 min. The mixture was prepared with Aerosil R805, 8.83/100 g (ESO + THPE-GE) and degassed for 15 min at 55 °C. Designated flax fiber was added to the mixture with mechanical stirring for 15 min. After the mixture cooled to room temperature, curing agent was added with mechanical stirring and then transferred into the mold (115 mm × 115 mm × 3 mm). Pressure was applied to the mold by a press of 5000 lb at 100 °C for 1 h. The mold was placed in an oven at 100 °C for 24 h for curing. The molded sheet was knocked out and further cured at 140 °C for 48 h. The cured sheets

[☆] Mention of trade names or commercial products in this [article] [publication] is solely for the purpose of providing specific information and does not imply recommendation or endorsement by the U.S. Department of Agriculture.

^{*} Corresponding author. Tel.: +1 309 681 6104; fax: +1 309 681 6340.

E-mail address: liuz@ncaur.usda.gov (Z. Liu).

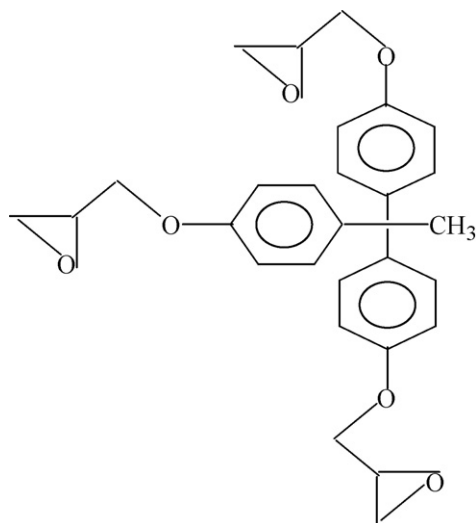


Fig. 1. Chemical structure of THPE-GE.

were cut to 75 mm × 10 mm × 3 mm for mechanical testing.

The nanocomposites were prepared by mixing ESO with Cloisite 30B particles at 60 °C for 2 h using a mechanical stirrer. The mixture was sonicated at 60 °C for 2 h, followed by degassing for 30 min. Designated amount of triethylenetetramine (TETA) was added to the pre-mix at room temperature with stirring, followed by degassing at 60 °C for 15 min. The mixture was poured into a container made from transparency film, and cured in an oven at 60 °C for 16 h, then at 120 °C for 48 h.

2.2. Mechanical testing

2.2.1. Tensile tests

The nonlinear mechanical behavior of the fibrous/soybean oil-based composites is analyzed using an Instron model IX automated materials testing system in tensile mode, with a load cell of 1000 N capacity. The cross-head speed is 50 mm/min. The specimen is a thin rectangular strip (75 mm × 10 mm × 3 mm). Tensile tests are performed at 25 °C. The values reported in this study are the average of five measurements. Standard deviation range is ±5% on strength and modulus. For nanocomposites, the dumbbell-shaped specimen is used, which has a gauge section with a length of 33 mm, a width of 6.35 mm and a thickness of around 4.5 mm.

2.2.2. Bending tests

Three-point bend tests are carried out at room temperature with a cross-head speed 25 mm/min and a span of 40 mm.

2.3. Characterizations of composites and nanocomposites

Scanning electron microscopy (SEM) was performed to investigate the interface between the filler and the polymeric matrix with a JEOLJSM 6400V instrument. The micrographs were obtained using 5 kV of accelerating voltage.

Powder X-ray diffraction (XRD) analysis was performed using a Philips 1830 diffractometer operated at 40 kV, 30 mA with graphite-filtered Cu K α (λ = 0.154 nm) radiation and a θ compensating slit. Data were acquired in 2θ = 0.05°, 4 s steps. The scanning range is from 2.5° to 10°. XRD was performed at room temperature.

Transmission electron microscopy (TEM) specimens were cut from nanocomposite blocks using an ultramicrotome (REICHERT OMU3 Ultramicrotome) equipped with a diamond knife. Transmission electron micrographs were taken with a JEOL, JEM 100C at an acceleration voltage of 100 kV.

3. Results and discussion

3.1. Flax fiber-reinforced composites

3.1.1. Morphology

SEM image in Fig. 2 shows the fractured surface for the composite filled with flax fiber (fiber length, 3.63 mm). The fiber fraction is 10 wt.%. Micrograph clearly indicates a good interfacial adhesion between the fiber and matrix due to the physical contact between both components. The fibers are broken up from the matrix.

3.1.2. Effect of ESO/THPE-GE ratio

The experiments were carried out for investigating influence of ESO/THPE-GE ratio (by weight) on mechanical properties of the composites. The results presented in Table 1 show that flexural modulus increases as the THPE-GE concentration increases. This indicates that THPE-GE resin has a determining influence on mechanical properties of the composites. In the two-component matrix system, ESO is a soft segment, and THPE-GE resin is a hard segment. An increase in the THPE-



Fig. 2. SEM image of fractured surface of composites filled with flax fiber.

Table 1
Effect of ESO/THPE-GE ratio

ESO/THPE-GE ratio (weight)	Flexural modulus (GPa)	Flexural strength (MPa)	Strain at break (%)
1:0.23	0.66	125	3.4
1:0.33	0.67	127	1.6
1:0.43	0.94	129	1.7

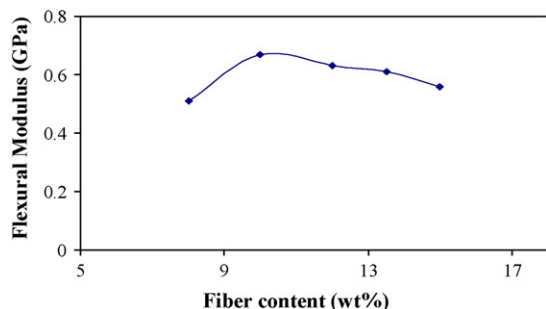


Fig. 3. Flexural modulus of composites as a function of flax fiber content.

GE resin concentration provides the composite with a higher flexural modulus.

3.1.3. Effect of fiber loading

The flexural modulus of composite as a function of flax fiber content is presented in Fig. 3. It is observed that at the lower fiber content (up to 10 wt.%) the flexural modulus increases from 0.51 to 0.67 GPa. However, at higher fiber loading (up to 15 wt.%), the flexural modulus shows a decrease. The highest flexural properties are achieved at about 10 wt.% fiber content. The decrease in the flexural properties at higher fiber contents is due to the increased fiber-to-fiber interactions and dispersion problems.

3.2. Clay-reinforced nanocomposites

3.2.1. Characterization of nanocomposites

The XRD patterns of the nanocomposites and the clay particle are shown in Fig. 4. The Cloisite 30B clay has a sharp peak at 4.5° . The peak corresponds to the [001] basal reflection of the organoclay. For the composites with 0, 5, 8 and 10 wt.% clay contents, no clear peaks were observed, suggesting that silicate layers of organoclay may be exfoliated in the polymer matrix. Although it is a common practice to classify a nanocomposite as fully exfoliated from the absence of (001) reflection, it is difficult to reach a definitive conclusion about the defined structure from the XRD alone. Thus, TEM techniques are necessary to characterize the composites. Fig. 5 shows a TEM image of ESO/clay nanocomposites containing 5 wt.% of clay. The dark lines in the figure correspond to the silicate nanolayers. TEM image shows that there was no aggregation of organoclay parti-

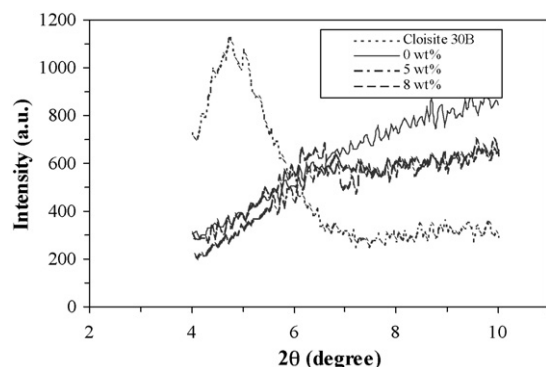


Fig. 4. X-ray diffraction of ESO/clay nanocomposite samples.

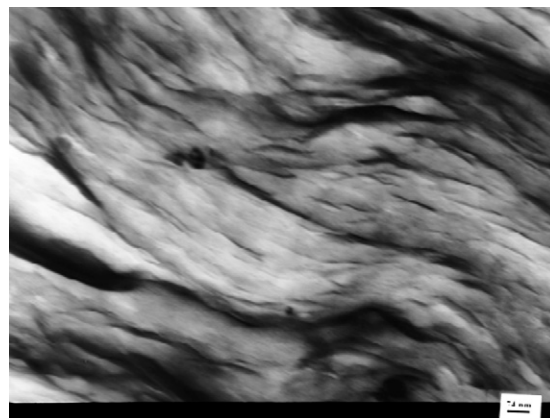


Fig. 5. TEM image of ESO/clay nanocomposite (clay, 5 wt.%).

cles. This suggests that the organophilic clay particles are well dispersed in the ESO matrix. Layer spacing of the clay in the nanocomposites increased, compared to the organoclay galleries about 2 nm. There was a distribution in basal spacings. A wide distribution in basal spacings may cause the absence of the 001 reflection. Under these conditions, it is clear that an intercalated structure of the composites was developed.

3.2.2. Dynamic mechanical behavior

Fig. 6 shows the dynamic mechanical spectra (dynamic storage modulus G' , and loss factor $\tan \delta$) as a function of temperature for ESO/clay nanocomposites with different clay loading. Some values of G' at various temperatures and T_g are presented in Table 2. The storage moduli initially remain almost constant at low temperatures between -30 and -10°C for all clay loading samples. The storage modulus of ESO/clay nanocomposites with 8 wt.% clay content shows a slightly higher value than other samples. As temperature increases to 0°C , the nanocomposite with 0 wt.% clay content shows lower storage modulus 154 MPa, than nanocomposites with 5 wt.% clay content 276 MPa. The nanocomposite with 8 wt.% clay content shows the highest value

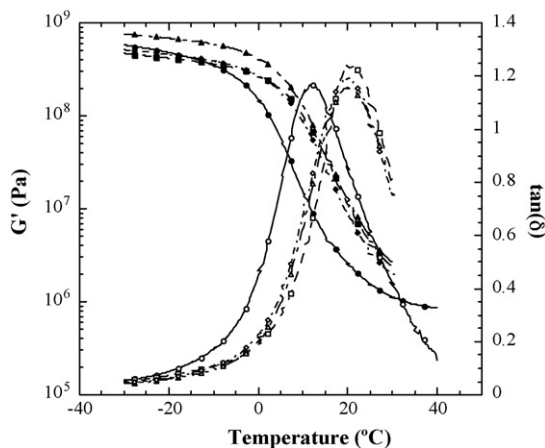


Fig. 6. The dynamic mechanical spectra as a function of temperature for the nanocomposites with different clay loading (filled symbols G' ; opened symbols $\tan \delta$; circle, 0 wt.% clay; square, 5 wt.% clay; triangle, 8 wt.% clay; diamond, 10 wt.% clay).

Table 2

Dynamic storage moduli of the ESO/clay nanocomposites at various temperatures

Cloisite 30B (wt.%)	Storage modulus, G' (MPa)				T_g (°C)
	−30 °C	0 °C	10 °C	30 °C	
0	590	154	16	1.1	11.8
5	500	276	108	2.5	20.7
8	763	415	128	2.7	19.4
10	520	275	88	2.0	20.2

Table 3

Tensile mechanical properties of the ESO/clay nanocomposites with different clay contents (epoxy/H ratio, 1:1.37)

Cloisite 30B (wt.%)	Tensile strength (MPa)	Young's modulus, E (MPa)	Percent elongation (%)
0	1.27	1.20	127
5	2.98	2.61	133
8	4.54	3.64	151
10	4.34	3.54	148

of 415 MPa. As the temperature increases further, the storage moduli of all samples drop, but samples with 0 wt.% clay loading drop sharply. Then this sample shows a modulus plateau after temperature of 25 °C, where the materials behave like a rubber. Apparently, the modulus drop corresponds to onset of segment mobility in the crosslinked polymer networks. The above results show clearly that the addition of clay up to 8 wt.% into ESO matrix results in a remarkable increase of stiffness. Increasing clay content to 10 wt.%, however, shows a decline in storage modulus.

The glass transition temperatures T_g of the ESO/clay nanocomposite obtained from the peak of the loss factor curve are presented in Table 2. It can be seen from Table 2 that the material with 0 wt.% clay content shows lower T_g , which is 11.8 °C, while that for the nanocomposite with 5 wt.% clay content is 20.7 °C. As the clay loading increases, the resulting nanocomposites show no significant difference in the glass transition temperature.

3.2.3. Tensile mechanical properties

The effects of the clay content on tensile properties of the nanocomposites are presented in Table 3. The tensile mechanical behavior of the nanocomposites greatly depends upon the clay

concentration. The tensile strength of nanocomposites increases rapidly from 1.27 to 4.54 MPa with increasing clay content from 0 to 8 wt.%. Similarly, the modulus increases rapidly from 1.20 to 3.64 MPa. A slight decrease in Young's modulus is observed when the clay content increases beyond 8–10 wt.%. The nanometric dispersion of silicate layers in matrix leads to improved modulus and strength. The stiffness of the silicate layers contributes to the presence of immobilized or partially immobilized polymer phases. It is also possible that silicate layer orientation as well as molecular orientation contributes to the observed reinforcement effects. The lower values of tensile strength and Young's modulus above 8 wt.% clay content can be attributed to the inevitable aggregation of the layers in high clay content.

4. Conclusions

From the above studies the following conclusion may be drawn. The ESO-based “green” composites and nanocomposites have been developed. The flexural modulus and tensile modulus of the composites increased proportionally with the amount of THPE-GE. The flexural modulus also increased with fiber contents lower than 10 wt.%, but showed a decrease beyond 10 wt.%. The tensile modulus increases with fiber content until a maximum, at 13.5 wt.%, and then it decreases.

XRD and TEM data indicate the organophilic clay is well dispersed in the matrix. An intercalated structure of the composite is developed. Dynamic mechanical study shows the ESO/clay nanocomposites with 5–10 wt.% clay content possess storage modulus ranging from 2.0 to 2.70 MPa at 30 °C. As T_g , about 20 °C was measured from a dynamic mechanical study. The mechanical study predicates these materials are promising as alternative to petrochemical polymers.

References

- [1] D.L. Kaplan, *Biopolymers from Renewable Resources*, Springer, New York, 1998.
- [2] J.A. Foulk, D.E. Akin, R.B. Dodd, Proceedings of 2000 Society of Automotive Engineers World Congress and Exposition, Detroit, Michigan, March 6–9, 2000, p. 2000-01-1133.
- [3] A. Usuki, M. Kawasumi, Y. Kojima, Y. Fukushima, A. Okada, T. Kurauchi, O. Kamigaito, *J. Mater. Res.* 8 (1993) 1179–1184.
- [4] Y. Kojima, A. Usuki, M. Kawasumi, A. Okada, Y. Fukushima, T. Kurauchi, O. Kamigaito, *J. Mater. Res.* 8 (1993) 1185–1189.